Catalysis Today 148 (2009) 389–397

Contents lists available at ScienceDirect

Catalysis Today

journal homepage: www.elsevier.com/locate/cattod

Effect of complexing agents of double metal cyanide catalyst on the copolymerizations of cyclohexene oxide and carbon dioxide

In Kyu Lee [a], Ju Young Ha [a], Chengang Cao [b], Dae-Won Park [a], Chang-Sik Ha [a], Il Kim [a,*]

[a] The WCU Center for Synthetic Polymer Bioconjugate Hybrid Materials, Division of Chemical Engineering, Pusan National University, Jangjeon-dong, Geumjeong-gu, Busan 609-735, Republic of Korea
[b] Department of Polymer Science and Engineering, Tianjin University of Science and Technology, Tianjin, China

ARTICLE INFO

Article history:
Available online 11 August 2009

Keywords:
Carbon dioxide
Catalysis
Copolymerization
Double metal cyanide
Epoxides
Polycarbonate

ABSTRACT

Copolymerizations of cyclohexene oxide (CHO) with carbon dioxide have been carried out by using a series of double metal cyanide (DMC) catalysts of the general formula, $Zn_3[Co(CN)_6]_2{\cdot}xZnX_2{\cdot}yH_2O{\cdot}z$[complexing agent (CA)], prepared by reacting $ZnClB_{2B}$ and $KB_{3B}[Co(CN)B_{6B}]B_2$ in the presence of *tert*-butyl alcohol as a main CA and various co-complexing agents (co-CAs) such as poly(tetramethylene ether glycol), polypropylene glycol, polyethylene glycol, poly(ethylene oxide)–poly(propylene oxide)–poly(ethylene oxide) triblock copolymer, and hyperbranched polyglycidol.The resulting DMC catalysts are characterized by elemental analysis, X-ray photoelectron spectroscopy, infrared spectroscopy, X-ray powder diffraction, thermal analysis and electron microscopy. The structure of DMC catalysts with an average size ranging from 183.3 to 294.2 nm changes from amorphous to crystalline based on the co-CA used. All catalysts show high copolymerization activities depending on the type of co-CA and polymerization parameters. The resultant copolymers are analyzed by using nuclear magnetic resonance spectroscopy, infrared spectroscopy, gel permeation chromatography, and thermal analysis. The amount of CO_2 fixation on the polymer backbone changes dramatically according to the type of co-CA used: i.e. carbonate content ranging between 0.14 and 0.63. The copolymers are characterized by moderate molecular weight (M_n = 5400–11,600) with narrow polydispersity index (<2.0). The copolymers bearing large amount of CO_2 in their backbone show glass transition temperatures between 70 and 100 °C.

1. Introduction

The fixation of CO_2 to polymeric materials for the application in industrial fields is one of the most valuable researches for the 21st century considering the environmental issues. Carbon dioxide is an ideal synthetic feedstock since it is abundant, inexpensive, nontoxic, and nonflammable. In this aspect, chemists and biologists have put their efforts to increase the utilization of CO_2 by producing such organic chemicals. The past three decades have witnessed the great progress in the fixation of CO_2 into polycarbonates since the innovative work of Inoue et al. [1,2]. To date, many excellent reviews in different period contributed by Kuran [3], Super [4,5], Darensbourg [6–10] and Kim [11] have made good description of this topic, where the importance of catalyst was never overestimated. Unfortunately, CO_2 is a highly oxidized and thermodynamically stable compound, and its utilization in redox reactions requires high-energy substances or electro-reductive processes. In order to avoid this barrier, it is required to find highly reactive metal catalysts. A variety of transition metal elements such as Ni, Pd, Pt, Co, Rh, Ir, Fe, Ru, Mn, Re, Cr, Mo, W, V, Nb, Ta, Ti, Zr and U, and non-transition elements such as Mg, Zn, Sn, Cu and Ag have been studied for the chemical fixation of CO_2 to valuable organic materials.

Double metal cyanide (DMC) compounds, $Zn_3[Co(CN)_6]_2{\cdot}xH_2O$, can be categorized as Prussian blue analogues and are the reaction products of a water-soluble metal salt (e.g. $ZnCl_2$) and a water-soluble metal cyanide salt (e.g. $K_3[Co(CN)_6]_2$). They are well-known catalyst for the polymerization of epoxides and the synthesis of propylene oxide based polyether polyols which are used in a wide range of polyurethane applications [12]. However, the pure DMC compounds prepared in the absence of complexing agent (CA) are not active for the polymerization of epoxides [13]. Generally, organic CAs such as alcohols and/or co-complexing agents (co-CAs) are incorporated into the catalyst matrix to make them active. In this sense, the choice of CA and co-CA is one of the key parameters in designing active catalysts for epoxide polymerizations.

Recently Qi and coworkers reported that the copolymerization of propylene oxide [14] cyclohexene oxide [15] with carbon dioxide was successfully carried out by using DMC catalysts based

* Corresponding author. Tel.: +82 51 510 2466; fax: +82 51 513 7720.
E-mail address: ilkim@pusan.ac.kr (I. Kim).

0920-5861/$ – see front matter © 2009 Elsevier B.V. All rights reserved.
doi:10.1016/j.cattod.2009.07.073

on $Zn_3[Co(CN)_6]_2$. We have shown that the DMC catalysts of the representative molecular formula, $ZnB_{2.3}Cl_{1.0}[Co(CN)_6]_{1.0}{\cdot}2.0\ ^tBuOH{\cdot}1.0H_2O$, are active for the copolymerizations of epoxides and CO_2, yielding aliphatic polycarbonates that are biodegradable [16–18]. This hopeful result guides us to investigate the DMC catalysts in more detail for epoxides/CO_2 copolymerizations, by changing the catalyst composition emphasizing the type of co-CA employed. The DMC catalysts characterized by elemental analysis, X-ray photoelectron spectroscopy, infrared spectroscopy, X-ray powder diffraction, thermal analysis and electron microscopy were applied for cyclohexene oxide (CHO)/CO_2 copolymerizations under various parameters. In addition the resulting aliphatic polycarbonates were analyzed by nuclear magnetic resonance (NMR) spectroscopy, infrared (IR) spectroscopy, gel permeation chromatography (GPC), and thermal analysis.

2. Experimental

2.1. Materials

CHO monomer (from Aldrich) was distilled and stored over Linde type 4A molecular sieves. Carbon dioxide of 99.99% purity was used without further purification. Potassium hexacyanocobatate(III) ($K_3[Co(CN)_6]_2$), zinc chloride ($ZnCl_2$), tertiary butyl alcohol (^{t}BuOH), polyethylene glycol (PEG, molecular weight (MW) = 4800), and poly(ethylene oxide)–poly(propylene oxide)–poly(ethylene oxide) triblock copolymer $EO_{20}PO_{68}EO_{20}$ (P123) were purchased from Aldrich and used without further purification. Poly(tetramethylene ether glycol) (PTG, MW = 1800) and polypropylene glycol (PPG, MW = 3000) were donated by BASF Korea and SKC, respectively, and hyperbranched polyglycidol (HBP, MW = 3400) was synthesized according to the reported procedure [19].

2.2. Preparation of catalysts

The DMC catalyst of the molecular formula, $ZnB_{2.3}Cl_{1.0}[Co(CN)_6]_{1.0}{\cdot}2.0\ ^tBuOH{\cdot}1.0H_2O$ (**DMC-TBA**), bearing only ^{t}BuOH as CA was prepared according to the literature procedures [20].

The nano-sized DMC catalysts containing both CA (^{t}BuOH) and co-CA (PEG, PPG, PTMEG, P123 or HBP) were prepared by the similar protocol. For example, $K_3[Co(CN)_6]$ (0.6595 g, 2 mmol) solution dissolved in distilled water (20 mL) was added dropwise to $ZnCl_2$ (2.7258 g, 20 mmol) solution dissolved in distilled water (200 mL) containing PTG (2.9244 g, 2 mmol) at 80 °C under vigorous stirring and then the resulting mixture was kept stirring for 30 min at 80 °C. Then 50 mL of ^{t}BuOH was added to the resulting mixture and the mixture was stirred for 3 h at 80 °C. The mixture was centrifuged (6000 × *g*, 5 min) and the nano-sized solid cake was collected by decantation. The cake was washed with as aqueous ^{t}BuOH solution (50%) 3 times. The resulting nano-sized catalyst (**DMC-PTG**) bearing PTG as a co-CA was dried under vacuum for 6 h at 80 °C. Following the similar procedures, the DMC catalysts bearing PEG (**DMC-PEG**), PPG (**DMC-PPG**), P123 (**DMC-P123**) and HBP (**DMC-HBP**) were synthesized.

2.3. Copolymerization of cyclohexene oxide and carbon dioxide

Semi-batch copolymerizations of CHO with CO_2 were carried out in a 50 mL round-bottom glass reactor. The dried catalyst (10 mg) and 5 mL of CHO were added to the reactor under CO_2 flow at ambient temperature. After capping the reactor, the reactor was pressurized with CO_2 (typically 5 bar) by using syringe needle at a desired temperature. The pressure of CO_2 was kept as 5 bar during the copolymerization. After a certain period reaction time, unreacted CO_2 was completely released from the reactor to reduce pressure, terminating the copolymerization. The polymer powder was separated by precipitation using excess methanol, followed by filtration. The resulting polymer was dried under vacuum for 6 h at 80 °C before characterization. The yield of polymerization yield was determined by gravimetry.

2.4. Characterization

Scanning electron microscope (SEM) with energy dispersive spectrometer (EDS) was taken by HITACHI S-4800. Samples were coated with osmium. Particle size and size distribution analyses were performed on a dynamic light scattering (DLS, Malvern Zetasizer Nano ZS). X-ray diffraction (XRD) patterns of the catalysts were obtained with a RINT2000 wide angle goniometry 185 using Cu Kα radiation at 40 kV and 30 mA. X-ray photoelectron spectroscopy (XPS) analysis of the catalysts was performed on an ESCALAB 250 induced electron emission spectrometer with Al Kα (1486.6 eV, 12 mA, 20 kV) X-ray sources. The mid-infrared spectra of the catalyst from 3500 to 200 cm^{-1} were recorded using a Shimazu FT-IR 8400 Fourier transform interferometer equipped with a nichrome wire source, Ge/CsI beamsplitter and DTGS detector. Atmospheric water vapor was removed from the interferometer chamber by purging with dry nitrogen. Interferograms obtained after 128 scans were transformed by using a boxcar truncation function with a theoretical resolution of 1.0 cm^{-1}. ^{1}H NMR spectra of the polymers were performed on a Varian Gemini 2000 (300 MHz) spectrometer using $CDCl_3$ as a solvent. MW and polydispersity index (PDI) were recorded using a Waters 150-C instrument, operated at 35 °C, with a set at 103, 104 and 500 Å columns (tetrahydrofuran as a solvent). Differential scanning calorimetry (DSC) and thermogravimetric analysis (TGA) thermograms were recorded using a TA Instruments Q500 (10 °C/min) under nitrogen atmosphere.

3. Results and discussion

3.1. Preparation DMC catalysts

Prussian blue ($Fe_4[Fe(CN)_6]_3{\cdot}14H_2O$), one of the oldest known coordination solids is readily synthesized by the addition of ferric ions to an aqueous solution containing ferrocyanide ions:

$$4[Fe(H_2O)_6]^{3+} + 3[Fe(CN)_6]^{4-} \rightarrow Fe_4[Fe(CN)_6]_3{\cdot}24H_2O \quad (1)$$

Here, water molecules coordinated to the ferric ions are displaced by nitrogen atoms from the ferrocyanide ions to generate linear Fe^{II}–CN–Fe^{III} bridges and an extended framework based on the face-centered cubic unit cell [21]. When confronted with cyanide as a ligand, wide selections of metal ions prefer to adopt octahedral coordination geometry. Consequently, reactions related to reaction (1) above can be used to produce a large family of solids with structures based on the cubic Prussian blue framework [21–23]. As precipitated from aqueous solutions containing no extraneous alkali metal salts, these Prussian blue analogues tend to possess neutral frameworks in which charge balance dictates the number of lattice vacancies.

The water-soluble metal salt preferably has the general formula MX_2 in which M is selected from the group consisting of Zn^{II}, Fe^{II}, Co^{II}, and Ni^{II}. In the formula, X is preferably an anion selected from the group consisting of halide, hydroxide, sulfate, carbonate, cyanide, oxalate, etc. The water-soluble metal cyanide salts used to make the Prussian blue analogue compounds preferably have the general formula $K_3M'(CN)_6$ in which M′ is selected from the group consisting of Co^{III}, Fe^{III}, Cr^{III}, and Ir^{III}. The water-soluble metal cyanide salt may contain one or more of these metals.

The resulting Prussian blue analogues possess structures based upon a simple cubic $M^{m+}[M'(CN)_6]^{n-}$ framework, in which octahedral $[M'(CN)_6]^{n-}$ complexes are linked via octahedrally coordinated, nitrogen-bound M^{m+} ions [21–23]. The Prussian analogue, especially prepared by the combination of $ZnCl_2$ with $K_3Co(CN)_6$, is also well-known catalyst for the polymerization of epoxides and the synthesis of propylene oxide based polyether polyols which are used in a wide range of polyurethane applications [12]. However, the pure Prussian blue analogues are not active for the polymerization of epoxides. Generally, organic CAs such

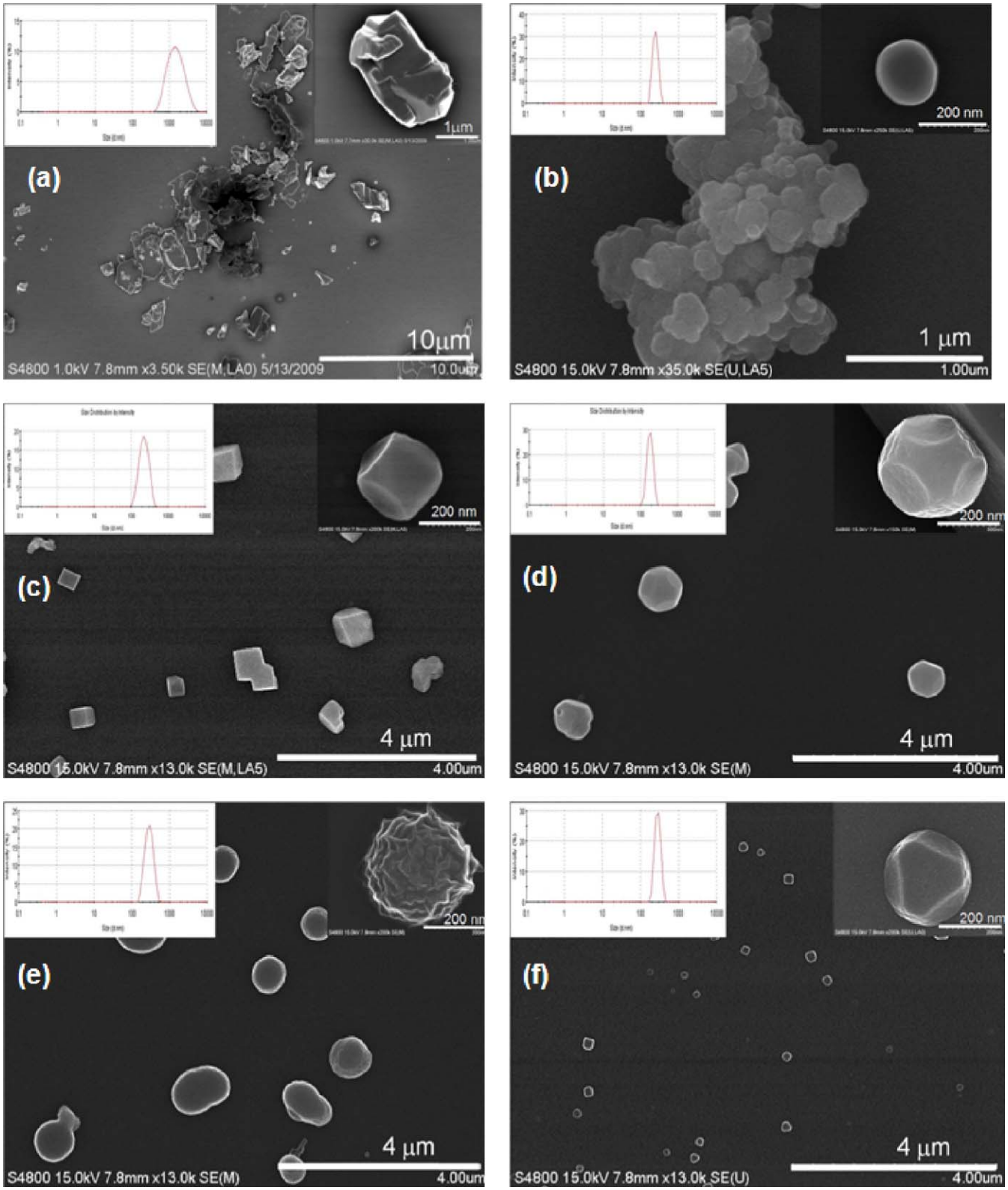

Fig. 1. SEM images of nano-sized double metal cyanide catalysts prepared in the presence of various polymeric co-complexing agents: (a) **DMC-TBA**, (b) **DMC-PEG**, (c) **DMC-PPG**, (d) **DMC-PTG**, (e) **DMC-P123**, and (f) **DMC-HBP**. Inset are particle size distribution curves measured by dynamic light scattering.

as alcohols and ethers are introduced into the catalyst matrix to make them active, even though the incorporation of the CAs makes the catalyst structure and formulation complicated.

For the preparation of highly active catalyst, excess amount of $ZnCl_2$ was reacted with $K_3Co(CN)_6$ in the presence of ^{t}BuOH as a CA, resulting in the DMC catalysts of the representative molecular formula, $Zn_{2.3}Cl_{1.0}[Co(CN)_6]_{1.0}\cdot 2.0\ ^t$BuOH$\cdot 1.0H_2O$ (**DMC-TBA**), which are active for the polymerizations of epoxides and the copolymerizations of epoxides with CO_2. The utilization of co-CA together with ^{t}BuOH enhances the catalytic activity [12,20]. In this study we have tried to achieve two targets at the same time by using co-CA: (1) the tune of the catalytic activity and (2) the control of the catalyst size by operating as a protecting agent. In fact, **DMC-TBA** catalyst prepared in the absence of co-CA yielded large and irregular particles (>1.5 μm) with very broad size distribution. However, aqueous $K_3Co(CN)_6$ solution were mixed with excess amount of aqueous $ZnCl_2$ solution containing co-CA ([Co]/[Zn]/[co-CA] = 1/10/1), readily producing a white colored suspension. The resulting mixture was treated with ^{t}BuOH and washed repeatedly with water, giving much smaller particles (<300 nm) with a narrow size distribution (Fig. 1). These results indicate that, during nucleation and growth processes of the DMC catalysts, the oxygen of hydroxyl moieties of the co-CAs are weekly coordinated to Zn and Co ions; consequently, the co-CA provided steric stabilization. Formation of the co-CA polymer protected DMC catalysts is schematized (Scheme 1).

It is interesting to note that the co-CA compounds function not only as a protecting agent to control the size of the catalyst

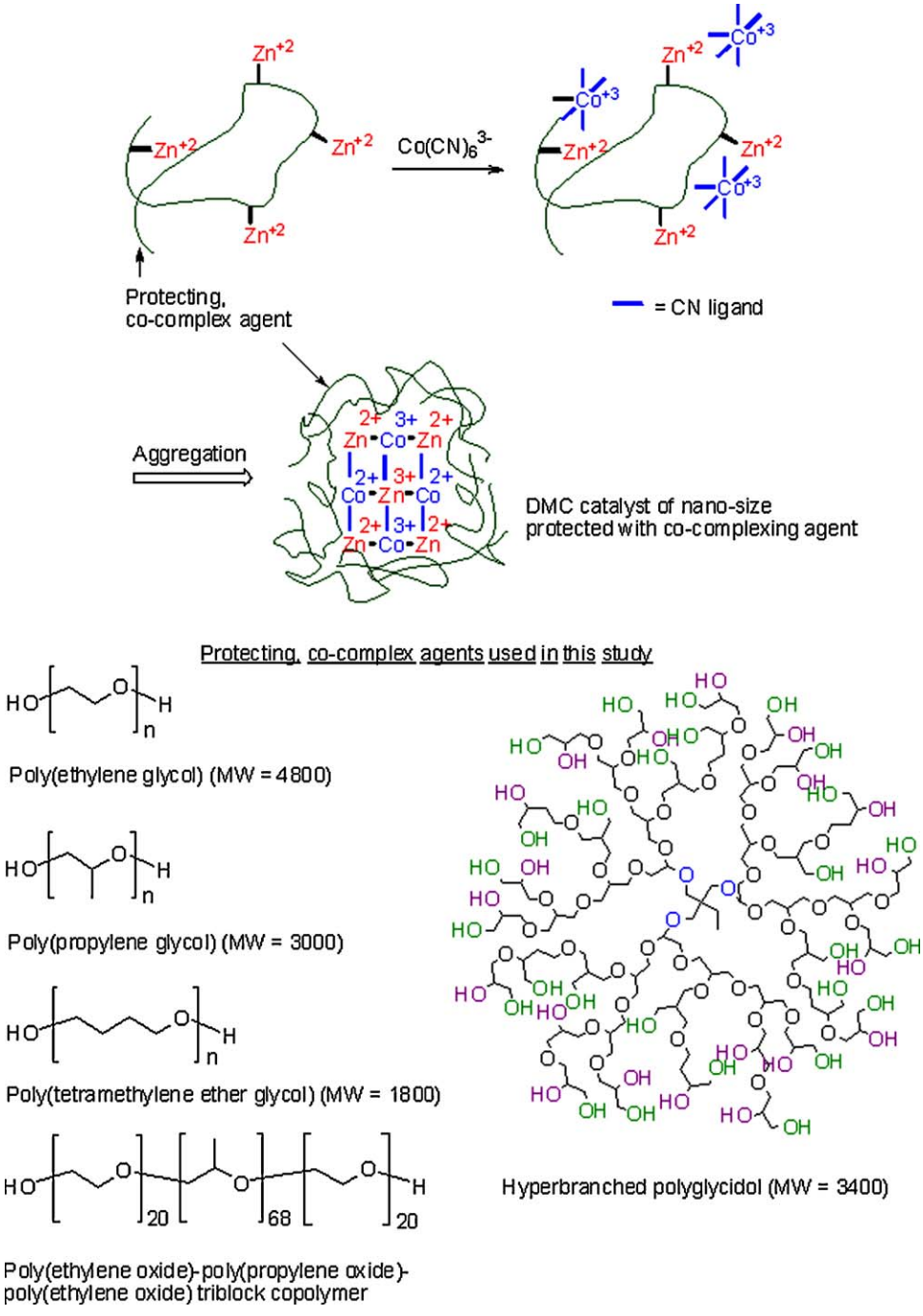

Scheme 1. Formation of the DMC catalysts protected by various co-complexing agents.

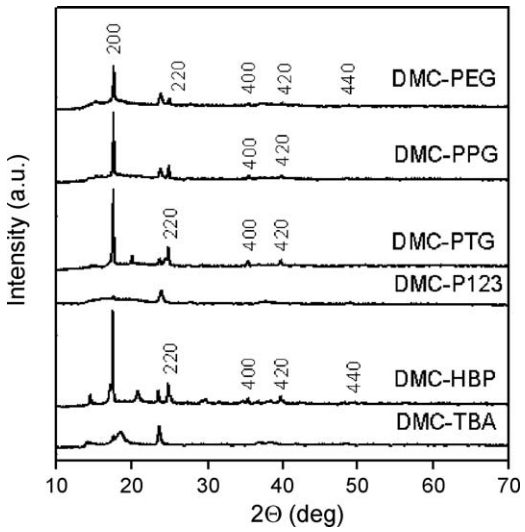

Fig. 2. XRD curves of the double metal cyanide catalysts prepared in the presence of various polymeric co-complexing agents such as poly(tetramethylene ether glycol) (PTG), polypropylene glycol (PPG), polyethylene glycol (PEG), poly(ethylene oxide)–poly(propylene oxide)–poly(ethylene oxide) triblock copolymer $EO_{20}PO_{68}EO_{20}$ (P123), and hyperbranched polyglycidol (HBP).

particles but as a co-CA possibly to enhance the catalytic activity and the CO_2 reactivity (*vide infra*). The average size of the catalyst particle could be controlled by the co-CA/Zn^{2+} feed ratio and the initial Zn^{2+} and Co^{2+} concentrations. At the same Zn^{2+} concentration, the sizes of the particles became smaller with an increase of co-CA content. However, as the size of DMC catalysts decreases, the amount of co-CA loaded to the catalyst matrix increases to an extent that the resulting catalysts show no activity in the polymerizations due to the excess amount of the co-CA. According to the screening tests inquiring the effect of catalyst size on the catalytic activity, the catalyst of the size around 200 nm showed the best results considering both catalytic activity and the easiness of the separation and handing. The mean diameters of **DMC-PTG**, **DMC-PEG**, **DMC-PPG**, **DMC-P123** and **DMC-HBP** are 183.3, 248.7, 228.6, 294.2, 284.8 nm, respectively (see insets in Fig. 1).

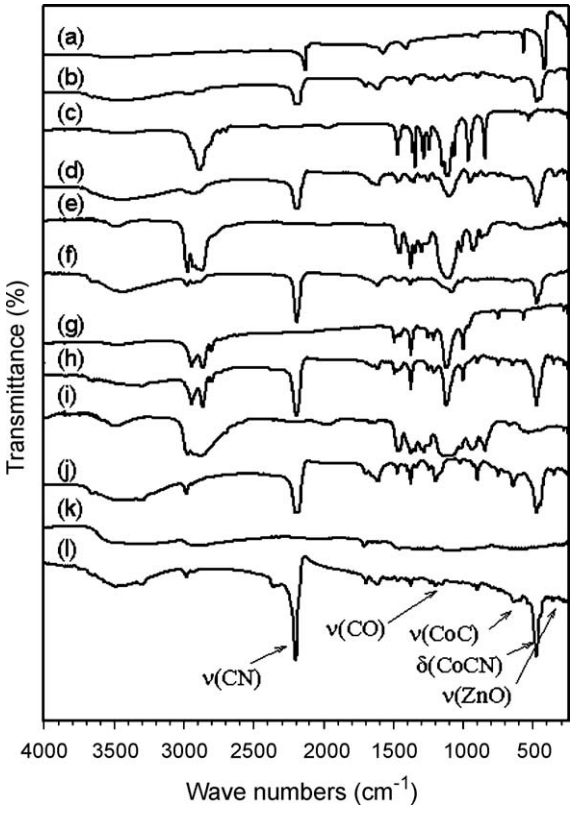

Fig. 3. Infrared spectra of (a) $K_3Co(CN)_6$, various co-complexing agents: (c) polyethylene glycol (PEG), (e) polypropylene glycol (PPG), (g) poly(tetramethylene ether glycol) (PTG), (i) poly(ethylene oxide)–poly(propylene oxide)–poly(ethylene oxide) triblock copolymer $EO_{20}PO_{68}EO_{20}$ (P123), and (k) hyperbranched polyglycidol (HBP), and the double metal cyanide catalysts prepared thereby: (b) **DMC-TBA**, (d) **DMC-PEG**, (f) **DMC-PPG**, (h) **DMC-PTG**, (j) **DMC-P123**, and (l) **DMC-HBP**.

3.2. Characterization of catalyst

X-ray powder diffraction analysis of the Prussian blue analogues of $Zn_3[Co(CN)_6]_2{\cdot}12H_2O$, prepared by equimolar amounts of aqueous $ZnCl_2$ and $K_3Co(CN)_6$ solutions in the absence of any complexing agents, showed broad peaks at 17.6° (2 0 0), 24.8° (2 2 0), 35.2° (4 0 0), 39.6° (4 2 0), 43.5° (4 2 2), which can be indexed as the Prussian blue cubic space group *Fm*3*m* [24]. However, the DMC catalysts prepared in the presence of ^{t}BuOH and ^{t}BuOH/co-CA showed much broader peaks and some of the characteristic peaks were disappeared (Fig. 2), demonstrating poorly crystalline structures. These results are most probably induced by the complexation of CA and co-CA to the catalyst matrix, and by the non-equivalent amount of Zn to Co. Note that excess amount of Zn ([Zn]/[Co] = 10) was used for the preparation of the catalyst to enhance the catalytic activity via pre-screening tests. Generally **DMC-TBA**, **DMC-PEG**, **DMC-PPG**, and **DMC-PTG** catalysts show relatively higher crystallinity than **DMC-P123** and **DMC-HBP** catalysts, in which no conspicuous peaks found in $Zn_3[Co(CN)_6]_2{\cdot}12H_2O$ compound. The crystallinity of the catalyst might influence the catalytic activity to some extent. Indeed, the highly crystalline $Zn_3[Co(CN)_6]_2{\cdot}12H_2O$ compound showed no activity in the epoxide polymerizations.

The IR spectra of the DMC catalysts exhibited characteristic peaks attributed to the C≡N stretching in the Zn^{2+}–CN–Co^{3+} of the DMC catalysts, the C–O stretching of ether unit in the CA and co-CA, and the –OH stretching vibration especially for **DMC-HBP** (Fig. 3 and Table 1). Cyano complexes can be identified easily since they exhibit sharp ν(CN) at 2200–2000 cm^{-1}. The ν(CN) of free CN^- is 2080 cm^{-1} (aqueous solution) [25]. Coordination to the metal shifts the ν(CN) to higher frequencies according to the electronegativity, the oxidation state, and the coordination number of metal. Thus, the ν(CN) band of $K_3Co(CN)_6$ was observed at 2131.3 cm^{-1} and the ν(CN) bands of the DMC catalysts prepared by the reaction of $ZnCl_2$ with $K_3Co(CN)_6$ in the presence of CA and co-CA shift further to 2191–2193 cm^{-1}. The ν(CN) shift to higher frequencies demonstrates that the CN^- ion acts as not only a σ-donor by donating electrons to the cobalt but also an electron donor by chelating to zinc metal. Electron donation tends to raise the ν(CN) since electrons are removed from the 5σ orbital, which is weakly antibonding, while π-back-bonding tends to decrease the ν(CN) because the electrons enter into the antibonding $2p\pi^*$

Table 1
Summary of the results of infrared spectroscopic analysis of the double metal cyanide catalysts.

Compound	D_p (nm)[a]	ν(Zn–O)	δ(Co–CN)	ν(Co–C)	ν(C–O)	ν(C≡N)
$K_3Co(CN)_6$		–	418.5	563.8	–	2127
DMC-TBA	1663.1	344.1	472.6	641.9	1095	2191
DMC-PEG	248.7	349.1	472.6	644.2	1097	2191
DMC-PPG	228.6	348.2	474.4	646.1	1087	2193
DMC-P123	183.3	349.1	472.6	644.2	1120	2191
DMC-PTG	294.2	339.5	470.6	642.2	1103	2193
DMC-HBP	284.8	339.5	472.6	645.4	1206	2191

[a] Average particle diameter measured by a dynamic light scattering.

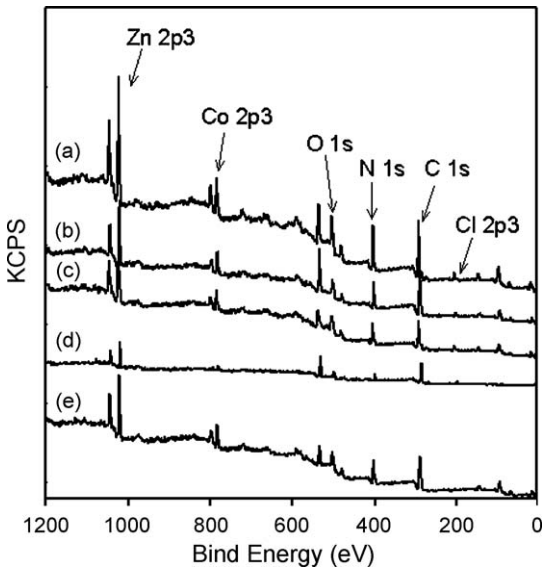

Fig. 4. XPS spectra of the double metal cyanide catalysts prepared in the presence of various polymeric co-complexing agents: (a) **DMC-PEG**, (b) **DMC-PPG**, (c) **DMC-PTG**, (d) **DMC-P123**, and (e) **DMC-HBP**.

orbital. In general, CN^{-1} is a good *s*-donor and a poorer *p*-acceptor. The C–O stretchings of CA and/or co-CA shift slightly by $\Delta\nu$ = 7–15. The degree of shift demonstrates that the CA compounds form very weak adducts, if any, with the DMC complexes.

In addition to ν(CN), the cyano complexes exhibit ν(Co–C) and δ(Co–CN) bands in the low frequency region (Table 1). The ν(Co–C) band in $K_3Co(CN)_6$ shifts from 563.8 to 642.3 cm^{-1} for the DMC catalysts and the δ(Co–CN) band in $K_3Co(CN)_6$ shifts from 412.7 to 470.6–474.4 cm^{-1} for the DMC catalysts. These results indicate that the Co–C π-bonding of $K_3Co(CN)_6$ is increased by the formation of Zn^{2+}–CN–Co^{3+} complex, since the degree of Co–C π-bonding might be proportional to the number of *d*-electron in the F_{2g} electronic level. The formation of Zn–O adduct, in which the oxygen atoms come from ^{t}BuOH and/or co-CAs, is evidenced by the observation of ν(Zn–O) between 339.5 and 349.1 cm^{-1}. It should be note that this Zn–CA complexation is a necessary condition to get active catalyst for polymerization.

XPS is sensitive to detect the chemical composition of the surface structures so that it is a good tool to characterize insoluble catalysts. Fig. 4 shows XPS curves of the DMC catalysts together with the starting materials and Table 2 summarizes the results. Relative atomic percentage of each element on the surface obtained by the integration of the peaks agrees well with the results of elemental analysis. The binding energy of zinc atom (the 2p3 XPS line at 1023.7 eV) in $ZnCl_2$ shifted to lower values, between 1019 and 1022 eV for the DMC catalysts. These shifts are related to the formation of Zn^{2+}–CN–Co^{3+} complexes. As the electron withdrawing power of the ligands bound to Zn atom decreases due to the substitution of Cl for CN ligands and at the same time the coordination of complexing agents to coordinatively unsaturated Zn metal centers led to the chemical shift to lower values. It is noted that there exist considerable amounts of free zinc halides (as Cl 2p3) (0.5–4.04 at.%), because excess amount of $ZnCl_2$ ([Zn]:[Co] = 10:1) was used for the preparation of the DMC catalysts. Even though we have no direct evidences to explain the results, the existence of the free zinc halide was very important to get highly active catalysts, according to our screening tests. The C 1s peak coming from the carbon element was taken as an internal reference and its BE value set at 284.6 eV. Peak assigned to Co 2p3 in $K_3Co(CN)_6$ shifts from 781 eV to slightly lower binding energy by 1–2 eV for the catalysts. These red shifts of the binding energy indicate a change of microenvironments for the corresponding metal elements due to the formation of Zn^{2+}–CN–Co^{3+} complexes in the presence of CAs. The O/Zn ratio might be a measure of the CA loaded to the catalyst. **DMC-TBA** catalyst shows the highest O/Zn ratio (3.79), meaning relatively large amount of ^{t}BuOH is complexed in the catalyst matrix, and **TBA-PTG** the lowest O/Zn ratio (1.25). However, this estimation is not so exact because each co-CA contains different oxygen to compound ratio.

The amount of organic fragments in the catalysts could be roughly estimated by TGA method (Fig. 5). The TGA thermogram of $K_3Co(CN)_6$ containing no organic CA shows major weight loss between 250 and 300 °C, and only about 40% of weight loss is recorded at 800 °C. Since the catalysts contain CAs much more weight losses are observed. Even though the thermal stability around 250 and 400 °C is somewhat different each other, the weight loss at 800 °C decreases in the order of **DMC-HBP** (73.2%) > **DMC-PTG** (72.4%) > **DMC-P123** (70.3%) > **DMC-PPG** (60.9%) > **DMC-PEG** (56.9%) > **DMC-TBA** (55.8%). These results demonstrate that **DMC-HBP** catalyst contains the largest amount of CAs and **DMC-TBA** catalyst the least. The high polarity of HBP due to the multiple hydroxyl groups (see Scheme 1) might provide favorable sites for the metal ions to be solubilized easily, resulting in high loading of HBP in the catalyst matrix.

3.3. Copolymerizations of CHO and CO_2

The semi-batch copolymerizations of CHO and CO_2 using the DMC catalysts have been carried out at various conditions at 5 atm of CO_2. For the comparison polymerizations of CHO were also carried out at 80 °C for 4 h. The results are summarized in Table 3. The copolymerization activity [as turnover number (TON)] obtained at 80 °C for 4 h increases in the order of **DMC-HBP** (962 g-polymer/g-Zn) < **DMC-PTG** (1654 g-polymer/g-Zn) < **DMC-P123** (2035 g-polymer/g-Zn) < **DMC-PPG** (2255 g-polymer/g-Zn) < **DMC-TBA** (2382 g-polymer/g-Zn) < **DMC-PEG** (2621 g-polymer/g-Zn). The order of homopolymerization activity of CHO is quite different from that of copolymerization activity: i.e. **DMC-PTG** (3854 g-polymer/g-Zn) > **DMC-PPG** (3133 g-polymer/g-Zn) > **DMC-P123** (2798 g-poly-

Table 2
Characterization of nano-sized DMC catalysts by XPS spectra.

Compound	Zn 2p3[a]		Co 2p3		O 1s		N 1s		C 1s		Cl 2p		O/Zn
	BE (ev)	[AT] %	BE (ev)	[AT] %	BE (ev)	[AT] %	BE (ev)	[AT] %	BE (ev)	[AT] %	BE (ev)	[AT] %	
$ZnCl_2$	1023												
$K_3Co(CN)_6$			781										
DMC-TBA	1019	8.08	780	2.89	530	11.9	397	18.2	284.2	55.14	197.6	3.79	3.79
DMC-PEG	1019	8.3	779	2.87	530	12.07	397	20.9	284.6	51.83	197.7	4.04	1.45
DMC-PPG	1019	4.78	779	1.88	530	14.7	397	13.81	284.6	63.24	195.8	1.59	3.07
DMC-PTG	1018	4.72	777	3.51	527	12.63	397	21.04	284.6	52.03	195.7	3.18	1.25
DMC-P123	1022	6.5	780	1.41	532	19.75	398	7.53	284.6	60.15	193.2	4.65	3.04
DMC-HBP	1021	6.5	780	2.67	532	10.22	399	21.99	284.6	58.13	194.6	0.5	1.57

BE: binding energy, AT: atomic ratio.

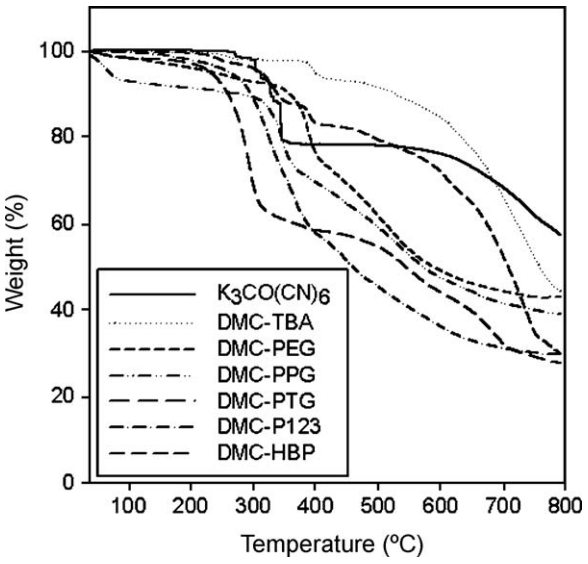

Fig. 5. TGA thermograms of the double metal cyanide catalysts prepared in the presence of various polymeric co-complexing agents such as poly(tetramethylene ether glycol) (PTG), polypropylene glycol (PPG), polyethylene glycol (PEG), poly(ethylene oxide)–poly(propylene oxide)–poly(ethylene oxide) triblock copolymer $EO_{20}PO_{68}EO_{20}$ (P123), and hyperbranched polyglycidol (HBP).

mer/g-Zn) > **DMC-PEG** (2680 g-polymer/g-Zn) > **DMC-TBA** (2648 g-polymer/g-Zn) > **DMC-HBP** (1254 g-polymer/g-Zn). For all catalysts, homopolymerization activity is higher than copolymerization activity. The reactivity of CO_2 [as the fraction of carbonate (f_{CO_2})] increases in the order of **DMC-PPG** (0.14) < **DMC-TBA** (0.18) < **DMC-P123** (0.35) < **DMC-PEG** (0.37) < **DMC-HBP** (0.63). Comparing to the results obtained by a homogeneous diethylzinc-based catalyst by Kuran [3] and Darensburg [7,8], and by chiral (salen)$Cr^{III}Cl$ complex, where H_2salen = N,N′bis(3,5-di-tert-butylsalicylidene)-1,2-cyclohexene diamine, by Darensburg [10], most of the DMC catalysts used in this study show higher activities, even though the reactivity of CO_2 is somewhat lower.

In order to investigate the effect of various experimental parameters on CHO/CO_2 copolymerization detailed polymerizations were carried out with **DMC-HBP** as a representative catalyst, considering it shows best CO_2 reactivity. The activity increases monotonously with an increase of catalyst concentration: i.e. rate of propagation (R_p) $\propto$ [cat], keeping the reactivity of CO_2 in a similar range ($f_{CO_2} = 0.63 - 0.66$). While the activity increases as the temperature increases from 80 to 120 °C, the reactivity of CO_2 decreases monotonously as the temperature increases, most probably due to the lower solubility of CO_2 at higher temperature. The copolymerizations at 100 °C at different period of time from 4 h to 12 h demonstrate that the activity increases as the reaction time increases. Through careful investigations of the copolymer products, we found no cyclic carbonate compound.

The results of homo- and copolymerization of CHO and CO_2 can be summarized as follows: (1) both the catalytic activity and the CO_2 reactivity are tunable simply by changing the type of co-CA; (2) it was impossible to get perfect alternating copolymer with $f_{CO_2} = 1.0$ by using the catalysts of the present study, indicating there exist considerable amounts of ether linkage in the backbone; and (3) both the catalytic activity and the CO_2 reactivity are also sensitive the experimental parameters such as temperature, catalyst amount, and polymerization time. Based on these polymerization results, we might propose the possible reaction modes applicable to the copolymerization of CHO and CO_2 utilizing DMC catalysts (Scheme 2). Pathway C producing cyclic carbonate and pathway C producing carbonate backbone are expected to be enhanced by a more electron-rich metal center, while pathway A affording ether linkages should be repressed under such circumstances. The electron-rich metal centers might be partly enhanced by the co-CA, resulting in conspicuous increase of f_{CO_2} values for some catalysts like **DMC-HBP**. The relative importance of pathway B over C is expected to be dependent on the steric and electronic environments of the metal center as well as the nature of the epoxide monomer. For example, copolymerizations of propylene

Table 3
Results of homo- and copolymerization of cyclohexene oxide (CHO) and CO_2 by using various double metal cyanide catalysts prepared in the presence of various polymeric co-complexing agents: polymerization conditions: CHO = 5 mL, P_{CO_2} (25 °C) = 5 atm.

Run no.	Catalysts	Co-CA[a]	Cat. (mg)	Temp. (°C)	Time (h)	*TON*[b]	M_n[c] × 10^{-3}	*PDI*[c]	f_{CO_2}[d]
1	**DMC-TBA**	–	20	80	4	2648	6.7	1.23	–
2	**DMC-PEG**	PEG	20	80	4	2680	8.2	1.03	–
3	**DMC-PPG**	PPG	20	80	4	3133	7.9	1.08	–
4	**DMC-PTG**	PTG	20	80	4	3854	7.6	1.03	–
5	**DMC-P123**	P123	20	80	4	2798	8.0	1.09	–
6	**DMC-HBP**	HBP	20	80	4	1254	18.0	1.47	–
7	**DMC-TBA**	–	20	80	4	2382	5.4	1.31	0.18
8	**DMC-PEG**	PEG	20	80	4	2621	8.2	1.53	0.37
9	**DMC-PPG**	PPG	20	80	4	2255	5.4	1.12	0.14
10	**DMC-PTG**	PTG	20	80	4	1654	5.8	1.82	0.63
11	**DMC-P123**	P123	20	80	4	2035	11.6	1.63	0.35
12	**DMC-HBP**	HBP	20	80	4	962	10.9	1.37	0.63
13	**DMC-HBP**	HBP	3	140	4	140	10.1	1.39	0.66
14	**DMC-HBP**	HBP	5	80	4	252	8.5	1.50	0.65
15	**DMC-HBP**	HBP	10	80	4	490	9.2	1.39	0.65
16	**DMC-HBP**	HBP	20	90	4	905	8.0	1.82	0.56
17	**DMC-HBP**	HBP	20	100	4	1740	5.7	1.78	0.49
18	**DMC-HBP**	HBP	20	110	4	1909	4.2	1.91	0.41
19	**DMC-HBP**	HBP	20	120	4	2023	3.4	1.65	0.35
20	**DMC-HBP**	HBP	20	100	6	2357	5.8	1.71	0.46
21	**DMC-HBP**	HBP	20	100	8	2812	6.2	1.75	0.44
22	**DMC-HBP**	HBP	20	100	10	3251	6.5	1.75	0.42
23	**DMC-HBP**	HBP	20	100	12	3548	6.9	1.78	0.42

[a] Co-complexing agent used in the catalyst preparation procedures: PEG: polyethylene glycol; P123: poly(ethylene oxide)–poly(propylene oxide)–poly(ethylene oxide) triblock copolymer; PTG: poly(tetramethylene ether glycol); PPG: polypropylene glycol; HBP: hyperbranched polyglycidol.
[b] Turnover number in g-polymer/g-Zn.
[c] Data from GPC.
[d] [Carbonate]/([carbonate] + [ether]) ratio determined by ^{1}H NMR spectra.

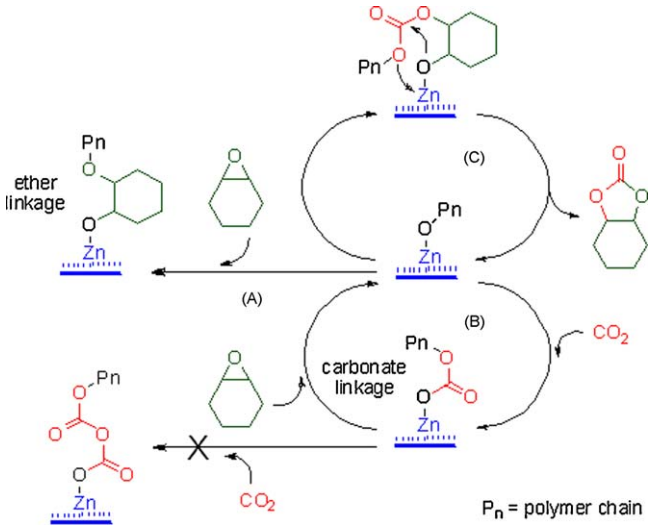

Scheme 2. Plausible pathways to form carbonate and ether linkage in the copolymerization of cyclohexene oxide (CHO) and CO_2 by using various double metal cyanide catalysts.

oxide and CO_2 produced considerable amount of cyclic carbonate compound. The polymerization results shown in Table 1 demonstrate that pathway A is also of importance for DMC catalysts. Current efforts are underway to examine a wide range of electronic and steric variations of the DMC catalysts, as well as the role of additives that can change the electronic environment of metal center on the kinetic parameters of the copolymerization of CHO and CO_2 to depress the pathway A leading undesired ether linkage.

3.4. Analysis of polymer

The extent of carbonate and ether backbone could be easily traced by IR and ^{1}H NMR spectrscopies of the copolymers. As is easily observed, the intense absorbance at approximately 1750 cm^{-1}, which corresponds to the asymmetric $\nu(CO_2)$ vibration of the copolymer (Fig. 6). Together with this, the existence of absorbance peaks around 1260 cm^{-1}, which is assigned to ether

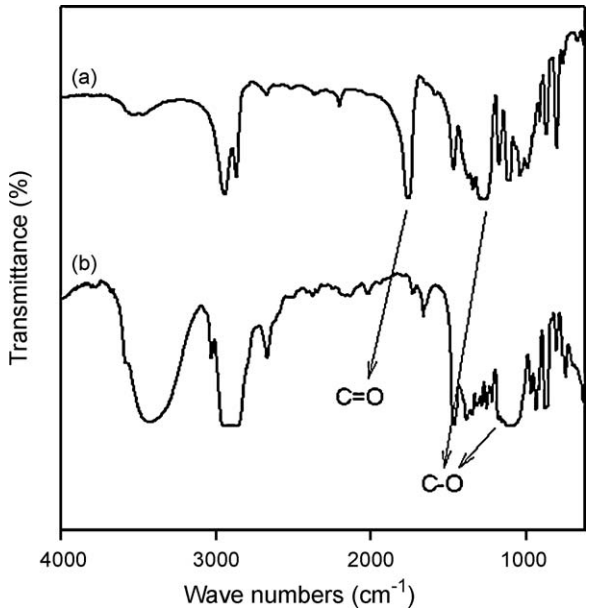

Fig. 6. IR spectra of polycarbonate (a) produced by using **DMC-HBP** catalyst at 80 °C and 5 bar of CO_2 for 4 h (run no. 12 in Table 3) and poly(cyclohexene oxide) (b) at similar conditions (run no. 6 in Table 3).

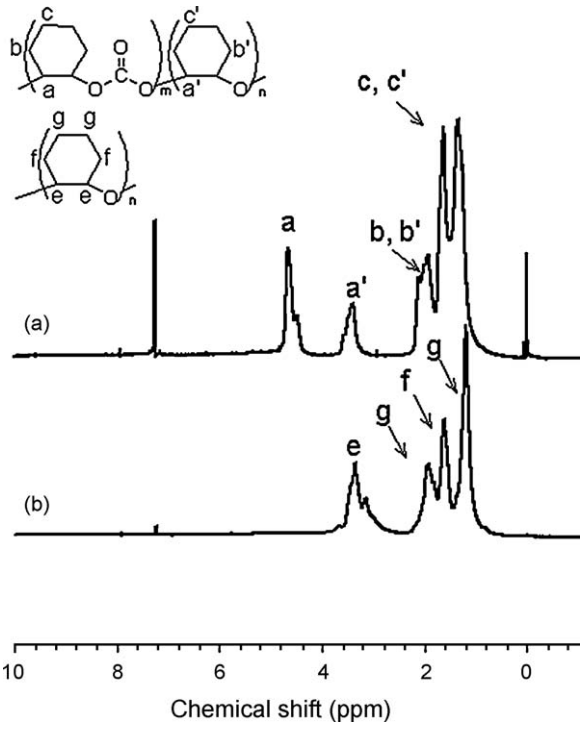

Fig. 7. ^{1}H NMR spectra of polycarbonate (a) produced by using **DMC-HBP** catalyst at 80 °C, 5 bar of CO_2 for 4 h (run no. 12 in Table 3) and poly(cyclohexene oxide) (b) at similar conditions (run no. 6 in Table 3).

ν(C–O) linkage, provides an evidence for the presence of both carbonate and ether backbone in the resultant copolymers. The absorbance corresponding to ν(C–O) linkage in CHO homopolymers appears at somewhat lower wavenumber (around 1080 cm^{-1}).

All isolated copolymers were subjected to ^{1}H NMR analysis in $CDCl_3$, and a representative spectrum of the copolymer produced by **DMC-HBP** catalyst at 80 °C is shown in Fig. 7, together with that of CHO homopolymer for the comparison. Percentage of carbonate linkage in the purified polymer (data shown in Table 3) was calculated from the relative intensities of the ^{1}H NMR signals corresponding to the methine protons next to the carbonate linkages (δ = 4.7 ppm) and ether linkages (δ = 3.4 ppm).

Analysis of the copolymer by gel permeation chromatography revealed the number average molecular weight ranges from 5400 to 11,600 g/mol for copolymers produced at 80 °C for 4 h of polymerization and from 6700 to 18,000 for poly(cyclohexene oxide) (PCHO) produced at similar conditions (Table 3). In general, homopolymers has higher molecular weight (MW) and narrower polydispersity index (PDI) than corresponding copolymers produced by the same catalyst at similar conditions. The PDI value of the homopolymers is ranging from 1.03 to 1.23 and that of copolymers from 1.12 to 1.82, when they are produced at 80 °C for 4 h. The MW value decreases as the temperature and the catalyst concentration increases with no mentionable trends in PDI value, while it increases monotonously as the time of polymerization increases together with slight increase of PDI value. It is interesting to note that the type of co-CA has a deep effect on the MW and PDI of the resulting homo- and copolymers as well as the polymerization behavior. The measured MW values do not match with those calculated for a living initiator based on the ratio of [*monomer*] to [*Zn*]. It is also assumed that some proportion of Zn metal should not be activated. These are suggestive of chain transfer and/or termination processes occurring in a complex manner. Detailed mechanistic study is ongoing in order to further figure out the

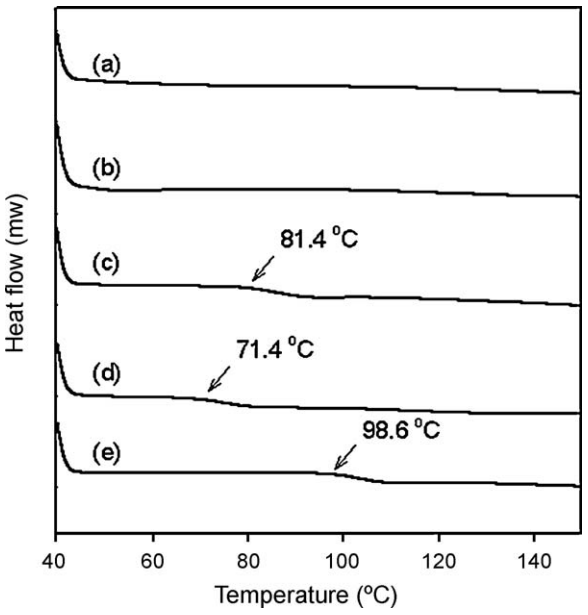

Fig. 8. DSC thermograms of the polymers produced by the copolymerizations of cyclohexene oxide and CO_2 at 80 °C, 5 bar of CO_2 for 4 h by using (a) **DMC-PEG**, (b) **DMC-PPG**, (c) **DMC-PTG**, (d) **DMC-P123**, and (e) **DMC-HBP**.

reason of very narrow PDI values, especially for the CHO homopolymerization.

DSC analysis of the copolymers (Fig. 8) produced at 80 °C shows that there were no conspicuous melting peaks between 25 and 200 °C, but some of copolymers bearing relatively large portion of CO_2 show glass transition temperature (T_g): i.e. 71.4, 81.4, and 98.6 °C, for the copolymer by **DMC-P123** ($f_{CO_2} = 0.35$), **DMC-PTG** ($f_{CO_2} = 0.63$), and **DMC-HBP** ($f_{CO_2} = 0.65$), respectively. These results indicate that the copolymers are not crystalline, which was also confirmed by XRD analysis of the copolymers, and the T_g values increase with the CO_2 amounts incorporated in the polymer backbone.

4. Conclusions

Semi-batch copolymerizations of CHO and CO_2 were carried out at moderate CO_2 pressure (5 bar) by using various DMC catalysts bearing different type of co-CAs. We have selected the co-CA to play 2 roles at the same time: i.e. as a CA and as a protecting agent to stabilize the catalyst particles of nano-size (183.3–294.2 nm) with different crystallinity. According to the copolymerizations at 80 °C for 4 h, **DMC-PEG** showed the best activity (2621 g-polymer/g-Zn) and **DMC-HBP** the best CO_2 reactivity ($f_{CO_2} = 0.63$). The copolymers were characterized by moderate MW values (M_n = 5400–11,600) with narrow polydispersity. The copolymers bearing large amount of CO_2 in their backbone show T_g between 70 and 100 °C.

Detailed copolymerizations investigated by using **DMC-HBP** catalyst, the activity and the resulting copolymer MW were sensitive to various parameters such as temperature, catalyst amount and polymerization time. Even though CO_2 reactivity was somewhat changed by the parameters, the choice of co-CA was the most important factor to tune it. In this sense, further efforts are underway to search for the more active DMC catalysts depressing the pathway leading undesired ether linkage by examining a wide range of electronic and steric variations, as well as the role of additives that can change the electronic environment of metal center.

Acknowledgements

This work was supported by the *World Class University Program* (No. R32-2008-000-10174-0), the *National Core Research Center Program* from MEST (No. R15-2006-022-01001-0), the *Industrial Technology Development Program* from MKE (Project No. 10031872), and the *Brain Korea 21 program* (BK-21).

References

[1] S. Inoue, H. Koinuma, T. Tsuruta, J. Polym. Sci. Polym. Lett. B7 (1969) 287.
[2] S. Inoue, H. Koinuma, T. Tsuruta, Makromol. Chem. 130 (1969) 210.
[3] A. Rokicki, W. Kuran, J. Macromol. Sci. Rev. Macromol. Chem. C21 (1981) 135.
[4] M. Super, E. Berluche, C. Costello, E.J. Beckman, Macromolecules 30 (1997) 368.
[5] M. Super, E.J. Beckman, Macromol. Symp. 127 (1998) 89.
[6] D.J. Darensbourg, M.W. Holtcamp, Macromolecules 28 (1995) 7577.
[7] D.J. Darensbourg, N.W. Stafford, T. Katsurao, J. Mol. Catal. A: Chem. 104 (1995) L1.
[8] D.J. Darensbourg, M.W. Holtcamp, G.E. Struck, M.S. Zimber, S.A. Niezgoda, P. Rainey, J.B. Robertson, J.D. Draper, J.H. Reibenspies, J. Am. Chem. Soc. 121 (1999) 107.
[9] D.J. Darensbourg, J.R. Wildeson, J.C. Yarbrough, J.H. Reibenspies, J. Am. Chem. Soc. 122 (2000) 12487.
[10] D.J. Darensbourg, J.C. Yarbrough, J. Am. Chem. Soc. 124 (2002) 6335.
[11] I. Kim, D.-W. Park, C.-S. Ha, J. Korean Ind. Eng. Chem. 137 (2002) 632.
[12] B. Le-Khac, EP 0,755,716 (1997).
[13] K.G. McDaniel, M.J. Perry, J.E. Hayes, WO 9,914,258 (1999).
[14] S. Chen, Z. Hua, Z. Fang, G. Qi, Polymer 45 (2004) 6519–6524.
[15] S. Chen, G. Qi, Z.-J. Hua, H.-Q. Yan, J. Polym. Sci. Part A: Polym. Chem. 42 (2004) 5284.
[16] I. Kim, M.J. Yi, K.J. Lee, D.-W. Park, B.U. Kim, C.-S. Ha, Catal. Today 111 (2006) 292.
[17] M.J. Yi, S.-H. Byun, C.-S. Ha, D.-W. Park, I. Kim, Solid State Ion. 31 (2004) 139.
[18] I. Kim, M.J. Yi, S.H. Byun, D.-W. Park, B.U. Kim, C.-S. Ha, Makromol. Chem., Macromol. Symp. 224 (2005) 181.
[19] A. Sunder, R. Hanselmann, H. Frey, R. Mulhaupt, Macromolecules 32 (1999) 4241.
[20] I. Kim, J.-T. Ahn, C.-S. Ha, C.S. Yang, I. Park, Polymer 44 (2003) 3417.
[21] H.J. Buser, A. Ludi, W. Petter, D. Schwarzenbach, J. Chem. Soc., Chem. Commun. (1972) 1299.
[22] A. Ludi, H.U. Güdel, Struct. Bond 14 (1973) 1.
[23] K.R. Dunbar, R.A. Heintz, Prog. Inorg. Chem. 45 (1997) 283.
[24] D.F. Mullica, G.W. Milligan, G.W. Beall, Acta Crystallogr. B34 (1978) 3558.
[25] K. Nakamoto, Infrared and Raman Spectra of Inorganic and Coordination Compounds, 3rd ed., Wiley, New York, 1978, p. 266.